Geothermics 81 (2019) 224–234

Contents lists available at ScienceDirect

Geothermics

journal homepage: www.elsevier.com/locate/geothermics

Analyzing transient heat and moisture transport surrounding a heat source in unsaturated porous media using the Green's function

Davood Yazdani Cherati[a], Omid Ghasemi-Fare[b,*]

[a] Department of Civil and Environmental Engineering, Sharif University of Technology, Tehran, Iran
[b] Department of Civil and Environmental Engineering, University of Louisville, Louisville, KY, United States

ARTICLE INFO

Keywords:
Energy pile
Analytical solution
Transient heat and moisture transport
Green's function

ABSTRACT

Generally, in most areas, groundwater level is deep and heat sources (e.g., energy piles) are embedded in unsaturated soil media. Therefore, in order to accurately analyze the soil response close to heat sources, both heat and moisture transport in unsaturated soil domain should be considered. Thermal loading changes the moisture content in the porous media. In this study, the energy conservation and mass fluid continuity equations derived from hydrothermal analysis of a partially saturated soil medium are considered in cylindrical coordinate system. To make the analytical solution possible, partial differential equations (PDEs) are turned into ordinary differential equations (ODEs), through linearization of the governing equations, and separation of variables. An analytical solution for the non-homogeneous system surrounding a heat source in unsaturated porous media is developed using Green's function. Energy piles are considered to be the heat source in this study. Results show the moisture transport in the soil medium depends on the duration of the thermal loading and relaxation time. Analytical results determine different influence zones for temperature and moisture content variations surrounding a heat source.

1. Introduction

Soil temperature increments close to heat sources (e.g., energy piles) alter the moisture content, and consequently changes the matric suction, and soil resistance parameters. Therefore, to determine the interaction of energy piles and surrounding soil, coupled thermo-hydro-mechanical analysis should be performed. Several researchers presented the coupled governing nonlinear partial differential equations for thermo-hydro-mechanical behavior of porous media (Gawin et al., 1996; Baggio et al., 1997; Gatmiri and Delage, 1997; Khalili and Loret, 2001; Wu et al., 2004). Among those, Gawin et al. and Khalili and Loret used the effective stress concept (Gawin et al., 1996; Khalili and Loret, 2001), Baggio et al. considered the derivations of thermodynamic equilibrium equations (Baggio et al., 1997), Gatmiri and Delage employed a new concept called thermal void ratio state surface (Gatmiri and Delage, 1997), and Wu et al. considered the thermal softening phenomenon (Wu et al., 2004) in order to drive the governing equations. According to literature, soil thermal displacements can be neglected in order to study the heat transfer mechanism in the ground and predict the soil temperature response. Heat conduction is commonly considered in literature as the major heat transfer mechanism in the ground surrounding energy piles. Eskilson and Claesson developed a model to predict the performance of heat pump systems in porous media (Eskilson and Claesson, 1988). Zeng et al. provided analytical solutions for the heat transfer from geothermal boreholes to the surrounding soil (Zeng et al., 2002, 2003). Lamarche and Beauchamp developed an analytical solution for the short time response of vertical boreholes (Lamarche and Beauchamp, 2007). Ghasemi-Fare and Basu presented a semi-analytical model to predict the energy efficiency of the energy piles considering variable inlet temperature (Ghasemi-Fare and Basu, 2013; Fare and Basu, 2013). In a separate study, they predicted the soil temperature response for both short term and long term close to the energy piles (Ghasemi-Fare and Basu, 2016). According to the results presented by Ghasemi-Fare and Basu, and Spilter et al., pore fluid flow alters the soil temperature response, and energy harvested from the ground (Ghasemi-Fare and Basu, 2018; Spitler et al., 2016). Only a few researchers studied both heat and moisture (fluid) flow in soil media close to the heat sources (e.g., energy piles). In one of the early studies Philip and De Vries analyzed the heat and moisture transport in undeformable soils (Philip and De Vries, 1957). De Vries developed differential equations derived by Philip and de Vries in 1957 for the heat and moisture transport in porous media under the combined effects of gravity, temperature gradient and moisture content (De Vries, 1958). Taylor and Cary presented a linear model to anticipate the

* Corresponding author.
E-mail addresses: Davood.Yazdani71@student.sharif.edu (D.Y. Cherati), Omid.ghasemifare@louisville.edu (O. Ghasemi-Fare).

https://doi.org/10.1016/j.geothermics.2019.04.012
Received 6 February 2019; Received in revised form 16 April 2019; Accepted 29 April 2019

Nomenclature

T	temperature
ρc	volumetric heat capacity of the porous medium
P	latent heat of vaporization
Q	a source term
ν	a negative constant
D_T	thermal moisture diffusivity
z	axial distance from the origin
a	radius of the energy pile
L	radius of the domain
G	Green's function
α	a separation constant
T_H	solution of the homogeneous energy conservation equation
J_0	the Bessel function of order 0 of the first kind
∇	the nabla operator
$f(r, z)$	initial condition for energy conservation equation
χ	the Lewis number
$\phi(x)$	an arbitrary function of x
$D_{\vartheta v}$	isothermal vapor diffusivity
λ	thermal conductivity
ρ	mass density
C	a constant
θ	volumetric water content
D_θ	isothermal moisture diffusivity
r	radial distance from the origin
h	height of the energy pile
H	height of the domain
*	the sign of dimensional variables
ξ	a separation constant
θ_H	solution of the homogeneous mass continuity equation
Y_0	the Bessel function of order 0 of the second kind
$\|\|\|$	indicating the norm of an eigenfunction
$g(r, z)$	initial condition for mass continuity equation
σ	a coefficient of the Posnov number
B_i	constant coefficients

heat and moisture movement in porous materials based on the theory of irreversible thermo-dynamics (Taylor and Cary, 1964). Thomas developed a two-dimensional model for heat and moisture transport by considering gravity effects in unsaturated soils (Thomas, 1985).

Governing partial differential equations of heat and mass transfer in both deformable and non-deformable porous media are generally nonlinear PDEs. Therefore, to make the analytical solution, possible simplified assumptions have to be considered. Using different techniques and considering the assumptions, the governing PDEs can be converted to linear equations and then closed form solution can be presented. These methods have always been key factors for developing accurate and practical results for preliminary design calculations (Selvadurai, 2007).

Recently, several researchers presented closed form solutions for the flow in the porous media (e.g., soil) at different conditions. Rockhold et al. presented an exact integral solution for the 1-D steady state vertical water flow in layered soils (Rockhold et al., 1997). Shao et al. developed a closed form solution considering both heat conduction and convection in soils using Fourier transformation (Shao et al., 1998). Pan provided the complete Green's function for multilayered and poroelastic half-space in isotropic condition (Pan, 1999). Taguchi and Kurashige developed the solutions for a 3-D infinite saturated porous media considering step-function forces and a transversely isotropic material (Taguchi and Kurashige, 2002). Gatmiri and Jabbari predicted the soil response for unsaturated deformable porous media with linear elastic behavior utilizing Green's function method for both 2D and 3D conditions (Gatmiri and Jabbari, 2005a,b). Chen and Ledesma presented a solution for a coupled heat and moisture transfer in waste repository in partially saturated clay barriers (Chen and Ledesma, 2007). Maghoul et al. used Laplace transformation and proposed a 3D analytical solution for the heat transport in an unsaturated deformable porous medium with linear elastic behavior (Maghoul et al., 2009). However, changes in moisture content in unsaturated soil close to geothermal piles/boreholes have not been completely studied in literature.

In this study, induced heat and moisture flow in non-deformable soil medium surrounding geothermal piles/boreholes are analytically analyzed. To provide the general solution different initial amount of water content can be considered. We provide a new solution method to study heat and moisture transport in unsaturated medium. The model provides exact closed form solution which can be used to: (1) better understand the heat and moisture transport in unsaturated soil media; and to (2) provide a validation tool for the numerical models. Note, the analytical solution has lower computational cost and can provide the general response. Partial differential equations provided by Philip and De Vries (Philip and De Vries, 1957) are solved in 2-D axisymmetric condition. An energy pile is considered to be as the heat source (heat generation term) in the porous medium in this model. Analytical solution is provided by separating the variables and using Green's function method. The advantages of the current method is providing a general solution which can consider various types of boundary conditions, initial conditions, and heat sources. The variations of temperature and water content with respect to time, depth and radius are studied thoroughly and the amounts of errors in this model are estimated.

2. Governing equations

The governing partial differential equations derived from hydrothermal analysis of non-deformable porous media presented by Philip and De Vries (Philip and De Vries, 1957) is simplified in the following equations.

2.1. Energy (heat) conservation equation

The energy (heat) equation governed by Fourier's Law is presented in Eq. (1).

$$\rho c\frac{\partial T_*}{\partial t_*} = \lambda\nabla^2 T_* - \rho P\nabla.\left(D_{\vartheta v}\nabla\theta_*\right) + Q_* \tag{1}$$

where T_* is temperature, $D_{\vartheta v}$ is the isothermal vapor diffusivity, ρc is the volumetric heat capacity of the porous medium, λ is the thermal conductivity, P is the latent heat of vaporization, ρ is the mass density and the subscript * stands for dimensional variables. Note, hydrostatic condition is assumed in this study and therefore the heat convection flow can be neglected.

The last term in the equation represents the evaporation term. Hartley and Black showed that the evaporation has very minimal effect on the soil temperature response in the domain (Hartley and Black, 1981), although it may depend on many parameters including permeability of the soil (Olivella and Gens, 2000). Therefore, in order to analytically solve the equation, the nonlinear evaporation term is neglected in this study. The energy conservation equation is presented in Eq. (2). As mentioned earlier, a heat generation term is considered to model the heat flux from the energy piles.

$$\frac{\partial T_*}{\partial t_*} = \frac{\lambda}{\rho c}\nabla^2 T_* + Q_* \tag{2}$$

where $Q_*\left[\frac{^\circ C}{s}\right]$ is the source term. The heat generation term depends on

the type of the heat source. It can be a constant or a function of time and space. In order to model the heat relaxation (recovery) period, an exponential function according to Eq. (3) can be considered as a heat source term.

$$Q_* = C_* \exp(\nu t) \tag{3}$$

In which $C_*\left[\frac{^\circ C}{s}\right]$ and ν are constant and ν is a non-positive number (zero represents a heating mode with constant source term, and a negative value represents the relaxation period). t is the dimensionless time.

For the negative value of ν heat generation term attenuates and reaches to zero. Considering such a heat source, it is expected that the soil temperature increases with time and reaches to a peak point and then drops to its initial value.

2.2. Mass fluid continuity equation

Mass continuity equation is governed by the Darcy's Law. The continuity equation can be written in terms of volumetric water content according to Eq. (4).

$$\frac{\partial \theta_*}{\partial t_*} = D_\theta \nabla^2 \theta_* + D_T \nabla^2 T_* \tag{4}$$

where θ_* is volumetric water content. D_T and D_θ are thermal and isothermal moisture diffusivity, respectively.

3. Boundary and initial conditions

Different source terms, non-homogeneous boundaries, and initial conditions can change the equilibrium state. Since the mass fluid continuity equation is linear, the effects of above mentioned parameters on the media can be individually studied. Then the effects of variations of parameters on soil temperature can be predicted using superposition theorem. Considering homogeneous initial and boundary conditions, the method of separation of variables can be used (Ã-zisik and Özışık, 1993). Note, mathematically an equation in which the right side is equal to zero can be defined as a homogeneous equation.

Fig. 1 shows the schematic geometry of the model including the energy pile. The geometry, boundary and initial conditions and the governing equations are symmetric with respect to the z axis. Therefore, PDEs are solved for the axisymmetric condition. Temperature, and volumetric water content at $r_* = L_*$ and $z_* = H_*$ are kept constant during the analysis, while heat source is placed at the center of the model (Lamarche, 2011; Gao et al., 2016; Li et al., 2005). Temperature, and moisture content at the top boundary are also kept constant during the analysis.

Boundary and initial conditions considered in this research are presented as below.

$$T_*(r_*, z_*, 0) = T_*(r_*, H_*, t_*) = T_*(L_*, z_*, t_*) = T_*(r_*, 0, t_*) = T_0 \tag{5}$$

$$\theta_*(r_*, z_*, 0) = \theta_*(r_*, H_*, t_*) = \theta_*(L_*, z_*, t_*) = \theta_*(r_*, 0, t_*) = \theta_0 \tag{6}$$

4. Theory and calculations

Green's function $G(r, z, t \mid r', z', \tau)$ estimates the variation of temperature with time at different locations (r, z), due to presence of point source load of unit strength, located at the point (r', z'), which releases thermal energy spontaneously at time $t = \tau$ (Ã-zisik and Özışık, 1993). Green's function is the response of the Dirac delta function. Therefore, integrating the product of Green's function and the generation term over the area of the source and over time (e.g., from τ to t), predicts the soil temperature surrounding a geothermal pile/borehole at time t. However, it is necessary to initially solve the homogenous equations. In order to solve the homogeneous PDEs, the method of separation of variables is used. This method predicts the exact solution for linear PDEs with homogeneous boundary conditions (Jeffrey, 2001). Ozisik explained this method in detail for the heat conduction equation (Ã-zisik and Özışık, 1993).

Dimensionless variables used in this study are defined as follows (Chen and Ledesma, 2007).

$$r = \frac{r_*}{a_*}, \quad z = \frac{z_*}{a_*}, \quad H = \frac{H_*}{a_*}, \quad L = \frac{L_*}{a_*}, \quad h = \frac{h_*}{a_*}, \tag{7}$$

$$t = \frac{D_\theta t_*}{a_*^2}, \quad T = \frac{T_* - T_0}{T_0}, \quad \theta = \frac{\theta_* - \theta_0}{\theta_0}, \quad \chi = \frac{\frac{\lambda}{\rho c}}{D_\theta}, \quad \sigma = \frac{T_0 D_T}{\theta_0 D_\theta},$$
$$C = \frac{C_* a_*^2}{D_\theta T_0} \tag{8}$$

where a_* and h_* are radius and height of the energy pile respectively, χ is the Lewis number which is the ratio of the heat diffusivity over the isothermal moisture diffusivity, σ is a coefficient of the Posnov number which is a ratio of the thermal moisture diffusivity over the isothermal moisture diffusivity.

Dimensionless PDEs, boundary and initial conditions are defined in Eqs. (9)–(13) using dimensionless variables:

$$\frac{1}{\chi}\frac{\partial T}{\partial t} = \nabla^2 T + Q \tag{9}$$

where

$$Q = C \exp(\nu t) \tag{10}$$

$$\frac{\partial \theta}{\partial t} = \nabla^2 \theta + \sigma \nabla^2 T \tag{11}$$

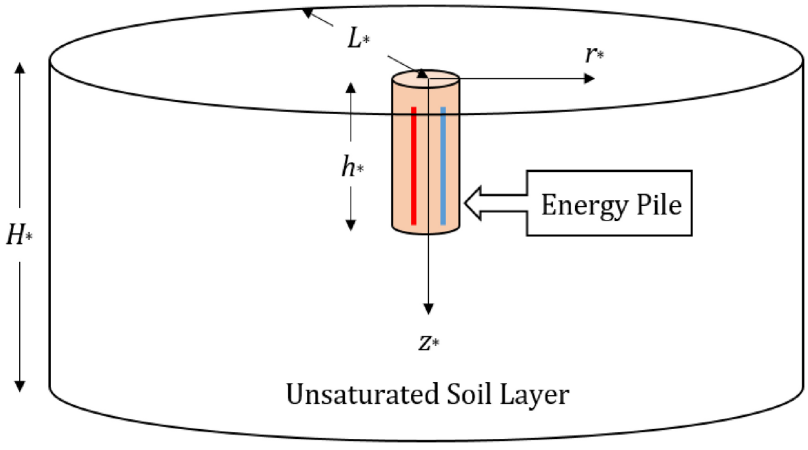

Fig. 1. Schematic geometry of the model including energy pile in an unsaturated soil layer.

$$T(r, z, 0) = T(r, H, t) = T(L, z, t) = T(r, 0, t) = 0 \tag{12}$$

$$\theta(r, z, 0) = \theta(r, H, t) = \theta(L, z, t) = \theta(r, 0, t) = 0 \tag{13}$$

The nabla operator in two-dimensional axisymmetric cylindrical coordinate system is defined in Eq. (14).

$$\nabla^2 = \frac{\partial^2}{\partial r^2} + \frac{1}{r}\frac{\partial}{\partial r} + \frac{\partial^2}{\partial z^2} \tag{14}$$

Eqs. (9) and (11) in cylindrical axisymmetric domain can be presented in Eqs. (15) and (16).

$$\frac{1}{\chi}\frac{\partial T}{\partial t} = \frac{\partial^2 T}{\partial r^2} + \frac{1}{r}\frac{\partial T}{\partial r} + \frac{\partial^2 T}{\partial z^2} + Q \tag{15}$$

$$\frac{\partial \theta}{\partial t} = \frac{\partial^2 \theta}{\partial r^2} + \frac{1}{r}\frac{\partial \theta}{\partial r} + \frac{\partial^2 \theta}{\partial z^2} + \sigma\left(\frac{\partial^2 T}{\partial r^2} + \frac{1}{r}\frac{\partial T}{\partial r} + \frac{\partial^2 T}{\partial z^2}\right) \tag{16}$$

4.1. Solution for energy conservation equation

In order to obtain the Green's function, the homogeneous energy conservation equation presented in Eq. (17) should be solved.

$$\frac{1}{\chi}\frac{\partial T}{\partial t} = \frac{\partial^2 T}{\partial r^2} + \frac{1}{r}\frac{\partial T}{\partial r} + \frac{\partial^2 T}{\partial z^2} \tag{17}$$

The solution procedure is commenced with assuming a separation of variables with respect to time and locations for the homogeneous equation. The separation of variables is presented below:

$$T_H(r, z, t) = T_1(r, z)\Gamma(t) \tag{18}$$

where T_H is the solution of the homogeneous equation.

By combining Eqs. (17) and (18) the general PDE can be expressed as:

$$\frac{1}{T_1}\left(\frac{\partial^2 T_1}{\partial r^2} + \frac{1}{r}\frac{\partial T_1}{\partial r} + \frac{\partial^2 T_1}{\partial z^2}\right) = \frac{1}{\chi}\frac{1}{\Gamma}\frac{d\Gamma}{dt} = -\alpha^2 \tag{19}$$

where α is a separation constant and will be calculated further.

The PDE with respect to time (t) is presented in Eq. (20).

$$\frac{d\Gamma}{dt} + \chi\alpha^2\Gamma = 0 \rightarrow \Gamma(t) = e^{-\chi\alpha^2 t} \tag{20}$$

Then a new separation of variables for $T_1(r, z)$ is assumed as below

$$T_1(r, z) = R(r)Z(z) \tag{21}$$

$T_1(r, z)$ can be expressed by combining Eq. (21) with the original PDE.

$$\frac{1}{R}\left(\frac{d^2R}{dr^2} + \frac{1}{r}\frac{dR}{dr}\right) + \frac{1}{Z}\frac{d^2Z}{dz^2} + \alpha^2 = 0 \tag{22}$$

The aforementioned separation equations are solved in this study and particular solutions are obtained by applying boundary conditions.

$$\frac{1}{Z}\frac{d^2Z}{dz^2} = -\eta^2 \rightarrow \frac{d^2Z}{dz^2} + \eta^2 Z = 0 \rightarrow Z(\eta, z) = B_1\sin(\eta z) + B_2\cos(\eta z) \tag{23}$$

Where η is obtained using boundary conditions. Eq. (23) is a second order ODE with two independent solutions in the form of Sine and Cosine functions. Solving Eq. (23) and considering the boundary condition, the value of η in Eq. (24) can be predicted.

$$Z(0) = Z(H) = 0 \rightarrow \eta_n = \frac{n\pi}{H},\ Z(\eta, z) = \sum_{n=1}^{\infty}\sin\left(\frac{n\pi}{H}z\right) \tag{24}$$

and

$$\frac{1}{R}\left(\frac{d^2R}{dr^2} + \frac{1}{r}\frac{dR}{dr}\right) = -\beta^2 \rightarrow \frac{d^2R}{dr^2} + \frac{1}{r}\frac{dR}{dr} + \beta^2 R = 0$$
$$\rightarrow R(\beta, r) = B_3J_0(\beta r) + B_4Y_0(\beta r) \tag{25}$$

Eqs. (23) and (25) can be considered as Sturm-Liouville equations (Jeffrey, 2001).

Eq. (25) is the order 0 of the Bessel equation, and its solutions, $J_0(\beta r)$ and $Y_0(\beta r)$ are the Bessel functions of order 0 of the first and second kind, respectively. The amount of Bessel function of order 0 of the second kind at $r = 0$ is infinity (Jeffrey, 2001); however, temperature and volumetric water content are limited values. Therefore, the solution for Eq. (25) is a coefficient of first order Bessel function only ($B_4 = 0$).

Considering boundary condition at $r = L$, the unknown coefficient can be determined. Solving the governing equations for an axisymmetric domain discussed above results in no specific value for boundary conditions at $r = 0$.

$$R(\beta, L) = 0 \rightarrow \beta_m = \frac{Zero_m}{L} \rightarrow R(\beta, r) = \sum_{m=1}^{\infty} J_0\left(\frac{Zero_m}{L}r\right) \tag{26}$$

where $Zero_m$ is the mth zero of first order Bessel function.

The homogeneous solution is expressed as

$$T_H(r, z, t) = \sum_{n=1}^{\infty}\sum_{m=1}^{\infty} C_1\sin\left(\frac{n\pi}{H}z\right)J_0\left(\frac{Zero_m}{L}r\right)e^{-\chi\alpha^2 t}, \quad \alpha^2 = \beta^2 + \eta^2 \tag{27}$$

where C_1 can be predicted using initial condition.

$$C_1 = \int_0^L\int_0^H \frac{r'\sin\left(\frac{n\pi}{H}z'\right)J_0\left(\frac{Zero_m}{L}r'\right)f(r', z')dr'dz'}{\left\|\sin\left(\frac{n\pi}{H}z'\right)\right\|^2\left\|J_0\left(\frac{Zero_m}{L}r'\right)\right\|^2} \tag{28}$$

In which $f(r, z)$ expresses the initial condition and $\|\|$ indicates the norm of the eigenfunction. The square of the norm with respect to the weight function $I(x)$ for Strum-Liouville equation is defined in Eq. (29)(Jeffrey, 2001)

$$\|\phi(x)\|^2 = \int_{a_1}^{a_2} I(x)\phi^2(x)dx, \quad a_1 \le x \le a_2 \tag{29}$$

where $\phi(x)$ is an arbitrary function.

Therefore, the homogeneous solution becomes

$$T_H(r, z, t) = \sum_{n=1}^{\infty}\sum_{m=1}^{\infty}\int_0^L\int_0^H r'f(r', z')\left(\frac{\sin\left(\frac{n\pi}{H}z\right)J_0\left(\frac{Zero_m}{L}r\right)e^{-\chi\alpha^2 t}\sin\left(\frac{n\pi}{H}z'\right)J_0\left(\frac{Zero_m}{L}r'\right)}{\left\|\sin\left(\frac{n\pi}{H}z'\right)\right\|^2\left\|J_0\left(\frac{Zero_m}{L}r'\right)\right\|^2}\right)dr'dz' \tag{30}$$

According to Eq. (31) Green's function at $\tau = 0$ is obtained from homogeneous solution (Ã-zisik and Özışık, 1993).

$$T_H(r, z, t) = \int_0^L\int_0^H r'G_T(r, z, t|r', z', \tau)|_{\tau=0}f(r', z')dr'dz' \tag{31}$$

Ozisik has shown that Green's function $G(r, t\,|\,r', \tau)$ for the transient heat conduction can be determined from $G(r, t\,|\,r', 0)$ by substituting t with $(t - \tau)$ (Ã-zisik and Özışık, 1993). Therefore, the Green's function for energy conservation equation can be presented as

$$G_T(r, z, t|r', z', \tau) = \sum_{n=1}^{\infty}\sum_{m=1}^{\infty}\frac{\sin\left(\frac{n\pi}{H}z\right)J_0\left(\frac{Zero_m}{L}r\right)e^{-\chi\alpha^2(t-\tau)}\sin\left(\frac{n\pi}{H}z'\right)J_0\left(\frac{Zero_m}{L}r'\right)}{\left\|\sin\left(\frac{n\pi}{H}z'\right)\right\|^2\left\|J_0\left(\frac{Zero_m}{L}r'\right)\right\|^2} \tag{32}$$

where G_T is the Green's function for energy conservation equation.

Solution of the energy conservation equation is obtained by integrating the Green's function multiplies by source term over the entire domain from τ to t.

$$T(r,z,t)= \chi\int_{\tau}^{t} d\tau \int_{A} r' G_T(r,z,t|r',z',\tau)\,\mathrm{gen}(r',z',\tau)\,dA' = \sum_{n=1}^{\infty}\sum_{m=1}^{\infty} \chi \frac{\sin\left(\frac{n\pi}{H}z\right)J_0\left(\frac{\mathrm{Zero}_m}{L}r\right)C}{\left\|\sin\left(\frac{n\pi}{H}z'\right)\right\|^2 \left\|J_0\left(\frac{\mathrm{Zero}_m}{L}r'\right)\right\|^2} \times \int_{\tau}^{t} e^{-\chi\alpha^2(t-\tau)}e^{\nu\tau}d\tau \int_{A'} r' \sin\left(\frac{n\pi}{H}z'\right)J_0\left(\frac{\mathrm{Zero}_m}{L}r'\right)dA' \quad (33)$$

4.2. Solution for mass continuity equation

The same procedure as described above is used to solve mass continuity equation.

Homogeneous equation to predict the changes in moisture content can be expressed as:

$$\frac{\partial\theta}{\partial t} = \nabla^2\theta \quad (34)$$

By assuming new separation of variables, Eq. (35) can be considered.

$$\theta_H(r,z,t) = \theta_1(r,z)\Omega(t) \quad (35)$$

where θ_H is the solution of the homogeneous equation.

Combining Eqs. (34) and (35), the PDEs can be explained as

$$\frac{1}{\theta_1}\left(\frac{\partial^2\theta_1}{\partial r^2}+\frac{1}{r}\frac{\partial\theta_1}{\partial r}+\frac{\partial^2\theta_1}{\partial z^2}\right) = \frac{1}{\Omega}\frac{d\Omega}{dt} = -\xi^2 \quad (36)$$

where ξ is a separation constant.

Homogeneous solution is achieved by solving separated equations.

$$\frac{d\Omega}{dt}+\xi^2\Omega = 0 \rightarrow \Omega(t) = e^{-\xi^2 t} \quad (37)$$

Separation of variables for $\theta_1(r,z)$ is assumed and presented in Eq. (38)

$$\theta_1(r,z) = M(r)N(z) \quad (38)$$

Then, the equation for θ_1 becomes

$$\frac{1}{M}\left(\frac{d^2M}{dr^2}+\frac{1}{r}\frac{dM}{dr}\right)+\frac{1}{N}\frac{d^2N}{dz^2}+\xi^2 = 0 \quad (39)$$

Solution for the separated equations can be expressed in Eqs. (40)–(43)

$$\frac{1}{N}\frac{d^2N}{dz^2} = -\zeta^2 \rightarrow \frac{d^2N}{dz^2}+\zeta^2 N = 0 \rightarrow N(\zeta,z) = B_5\sin(\zeta z)+B_6\cos(\zeta z) \quad (40)$$

$$N(0)=N(H)=0 \rightarrow \eta_p = \frac{p\pi}{H},\ N(\zeta,z) = \sum_{p=1}^{\infty}\sin\left(\frac{p\pi}{H}z\right) \quad (41)$$

$$\frac{1}{M}\left(\frac{d^2M}{dr^2}+\frac{1}{r}\frac{dM}{dr}\right) = -\mu^2 \rightarrow \frac{d^2M}{dr^2}+\frac{1}{r}\frac{dM}{dr}+\mu^2 M = 0 \rightarrow R(\mu,r) = B_7J_0(\mu r)+B_8Y_0(\mu r) \quad (42)$$

$$M(L)=0 \rightarrow \mu_q = \frac{\mathrm{Zero}_q}{L},\quad M(\mu,r) = \sum_{q=1}^{\infty}J_0\left(\frac{\mathrm{Zero}_q}{L}r\right) \quad (43)$$

The homogeneous solution is:

$$\theta_H(r,z,t) = \sum_{p=1}^{\infty}\sum_{q=1}^{\infty} C_2\sin\left(\frac{p\pi}{H}z\right)J_0\left(\frac{\mathrm{Zero}_q}{L}r\right)e^{-\xi^2 t},\quad \xi^2=\mu^2+\zeta^2 \quad (44)$$

where C_2 can be predicted using the initial condition.

$$C_2 = \int_0^L\int_0^H \frac{r'\sin\left(\frac{p\pi}{H}z'\right)J_0\left(\frac{\mathrm{Zero}_q}{L}r'\right)g(r',z')\,dr'dz'}{\left\|\sin\left(\frac{p\pi}{H}z'\right)\right\|^2\left\|J_0\left(\frac{\mathrm{Zero}_q}{L}r'\right)\right\|^2} \quad (45)$$

while $g(r,z)$ indicates the initial condition.

The homogeneous solution can be presented as

$$\theta_H(r,z,t) = \sum_{p=1}^{\infty}\sum_{q=1}^{\infty}\int_0^L\int_0^H r'g(r',z')\left(\frac{\sin\left(\frac{p\pi}{H}z\right)J_0\left(\frac{\mathrm{Zero}_q}{L}r\right)e^{-\xi^2 t}\sin\left(\frac{p\pi}{H}z'\right)J_0\left(\frac{\mathrm{Zero}_q}{L}r'\right)}{\left\|\sin\left(\frac{p\pi}{H}z'\right)\right\|^2\left\|J_0\left(\frac{\mathrm{Zero}_q}{L}r'\right)\right\|^2}\right)dr'dz' \quad (46)$$

By comparing Eqs. (46) and (47), Green's function can be predicted according to Eq. (48) (Ã-zisik and Özışık, 1993).

$$\theta_H(r,z,t) = \int_0^L\int_0^H r'G_\theta(r,z,t|r',z',\tau)|_{\tau=0}g(r',z')dr'dz' \quad (47)$$

$$G_\theta(r,z,t|r',z',\tau) = \sum_{p=1}^{\infty}\sum_{q=1}^{\infty}\frac{\sin\left(\frac{p\pi}{H}z\right)J_0\left(\frac{\mathrm{Zero}_q}{L}r\right)e^{-\xi^2(t-\tau)}\sin\left(\frac{p\pi}{H}z'\right)J_0\left(\frac{\mathrm{Zero}_q}{L}r'\right)}{\left\|\sin\left(\frac{p\pi}{H}z'\right)\right\|^2\left\|J_0\left(\frac{\mathrm{Zero}_q}{L}r'\right)\right\|^2} \quad (48)$$

where G_θ is Green's function for mass continuity equation.

The solution for mass continuity equation can be obtained using Green's function.

$$\theta(r,z,t) = \int_{\tau}^{t}d\tau\int_A r'G_\theta(r,z,t|r',z',\tau)\,\mathrm{gen}(r',z',\tau)dA' \quad (49)$$

In which the generation term is

$$\mathrm{gen}(r,z,t) = \sigma\left(\frac{\partial^2T}{\partial r^2}+\frac{1}{r}\frac{\partial T}{\partial r}+\frac{\partial^2T}{\partial z^2}\right) \quad (50)$$

5. Validation

In order to validate the analytical approach we used in this study, the experimental observation in a vertical borehole ground heat exchanger model performed by Beier et al. (2011) is compared with the results obtained from the analytical solution. A sandbox of 18 (m) × 1.8 (m) × 1.8 (m) with a borehole at the center was used in the experiment. They placed a borehole in the center of the box and monitored the temperature increments close to the borehole wall, and away from the borehole. The constant heat input rate was considered in the model. The details of the experimental setup information are presented in Beier et al. (2011). The experimental observations are compared with the analytical solution with constant heat source. Physical parameters and dimensions are adopted from Beier et al. (2011). The heat source term Q is selected based on the temperature increments provided by Beier et al. (2011) at the borehole wall. Fig. 2 presents the

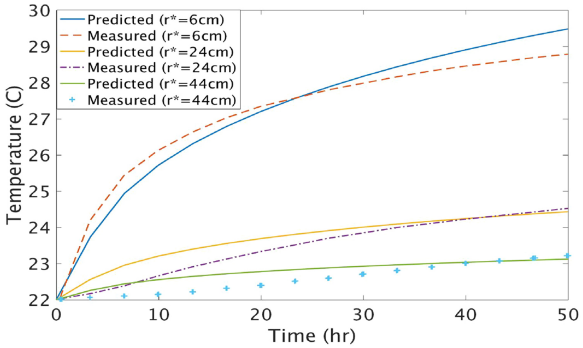

Fig. 2. Comparison of the temperature obtained from the analytical solution with experimental observations by Beier et al. (2011).

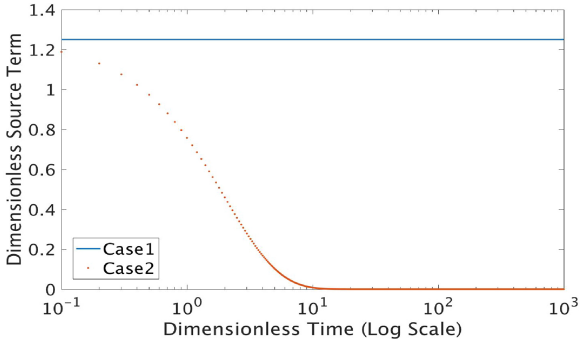

Fig. 3. Variation of the source term with time for both cases.

Table 1
Geometry, initial and boundary conditions.

a_* (m)	h_* (m)	L_* (m)	H_* (m)	C_* $\left(\frac{℃}{s}\right)$	T_0 (°C)	θ_0
1	15	50	50	5×10^{-5}	20	0.5

Table 2
Hydrothermal parameters of an unsaturated soil layer (Provided by Thomas (1985)).

$\frac{\lambda}{\rho C}$ $\left(\frac{m^2}{s}\right)$	D_T $\left(\frac{m^2}{s℃}\right)$	D_θ $\left(\frac{m^2}{s}\right)$
8×10^{-7}	10^{-9}	10^{-6}

Table 3
Dimensionless parameters resulted by Tables 1 and 2.

a	h	H	L	χ	σ	C
1.00	15.00	50.00	50.00	0.80	0.04	1.25

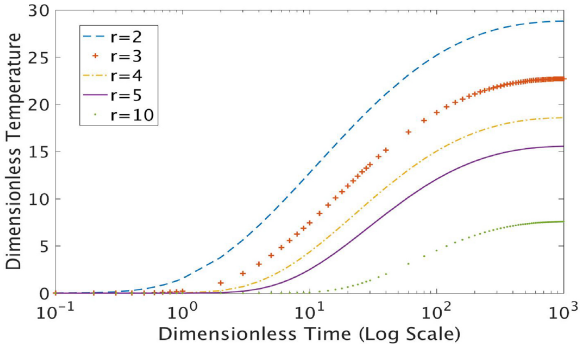

Fig. 4. Variation of temperature with time at $z = 10$ and five different radiuses for case 1.

comparison between the measured and predicted soil temperature increments at different radiuses from the borehole. As it can be seen in the figure, the predicted temperature using analytical method matches well with the experimental measurements. The difference between the recorded experimental data and predicted temperature is less than 0.5 °C (2% relative error).

6. Results and discussion

The proposed fundamental solution of the heat and moisture transfer in unsaturated soil media is used to analyze the heat and water flow surrounding a heat source. PDEs are solved for two different cases with constant and variable heat sources. Case 1 represents a constant heat source (same as the validation model) while heat source in case 2 attenuates. For the case 1: $\nu = 0$, and for case 2: $\nu = -0.5$. Fig. 3 shows

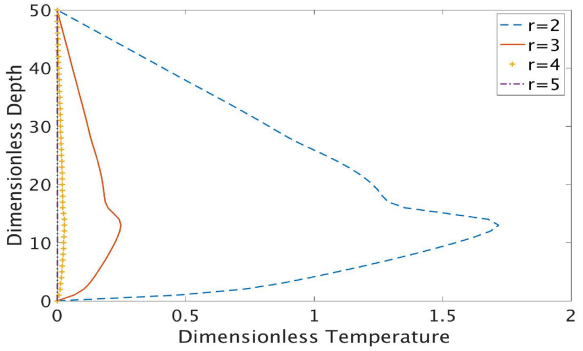

(a) At $t = 1$ and four different radiuses

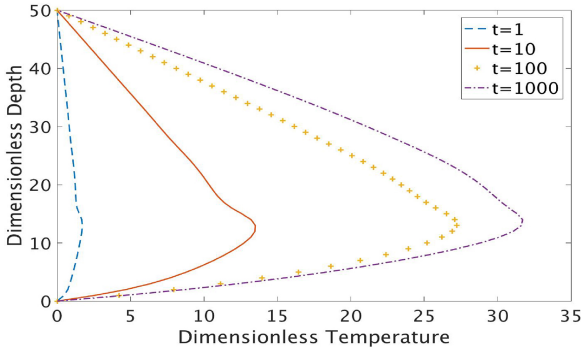

(b) At $r = 2$ and four different times

Fig. 5. Variation of temperature with depth for case 1.

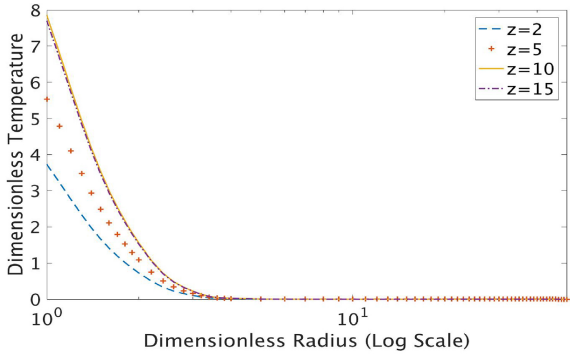

(a) At $t = 1$ and four different depths

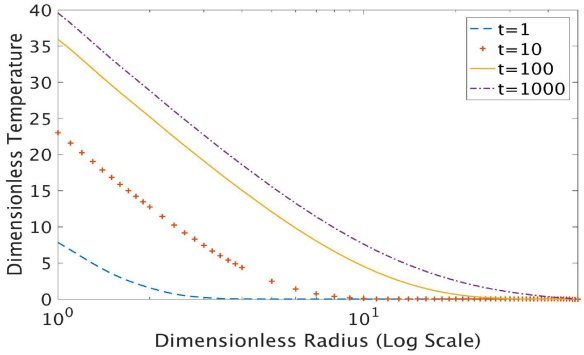

(b) At $z = 10$ and four different times

Fig. 6. Variation of temperature with radius for case 1.

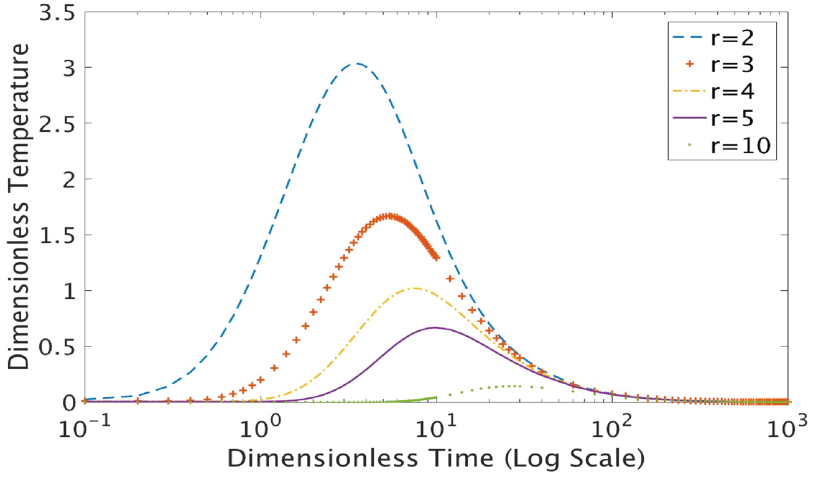

Fig. 7. Variation of temperature with time at $z = 10$ and five different radiuses for case 2.

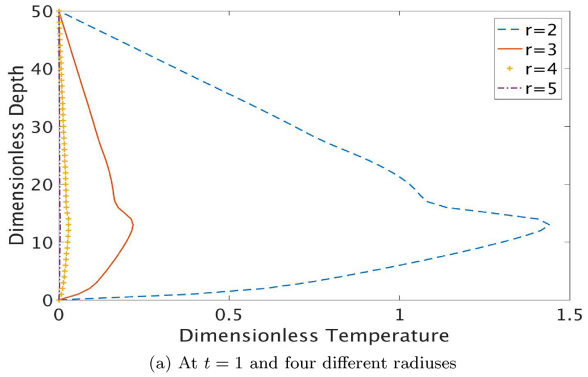

(a) At $t = 1$ and four different radiuses

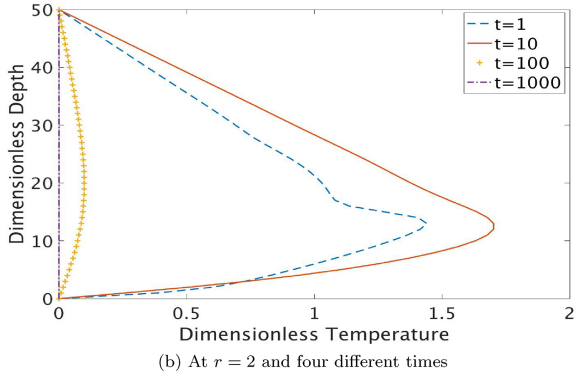

(b) At $r = 2$ and four different times

Fig. 8. Variation of temperature with depth for case 2.

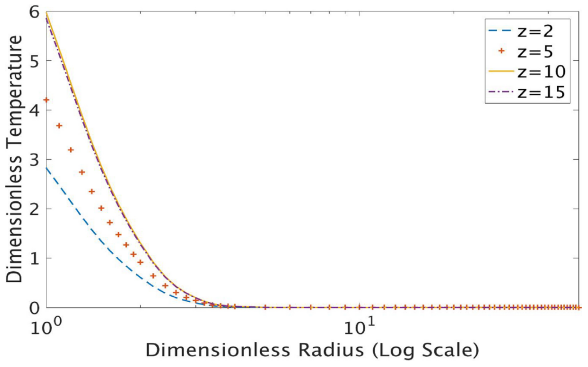

(a) At $t = 1$ and four different depths

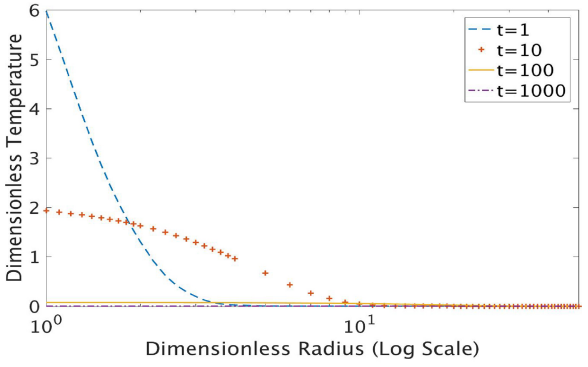

(b) At $z = 10$ and four different times

Fig. 9. Variation of temperature with radius for case 2.

the variation of source terms over time for both cases.

All parameters considered in this study are given in Tables 1–3. To present general solution, figures are presented based on dimensionless variables.

Fig. 4 shows the variation of temperature surrounding the heat source in time for case 1. According to the figure, temperature increases gradually with time, then reaches to the steady state condition and approaches to an asymptotic value. This is compatible with the results presented by Man et al. (2010) where they only considered heat flow in the soil surrounding an energy pile.

Dimensionless temperature variations along depth for case 1 and case 2 are presented in Figs. 5 and 8, respectively. Temperature changes in the ground surface is zero and then it gradually increases with depth and reaches to the maximum value at $z = 13$. Nearby the pile base, there is a drastic reduction in temperature increments. This reduction disappears over time. Dimensionless temperature finally reaches to zero at the bottom boundary. Figs. 5(a) and 8(a) present temperature evolution at different radius from the heat source considering constant and variable heat sources, respectively.

Figs. 6 and 9 show the variation of temperature with radius for two cases. As it can be seen in the figures, temperature decreases radially. Note, the influence zone (where the dimensionless temperature increment is at least 1) depends on the thermal operation time. The dimensionless influence zones are 3, 7 and 30 for the time steps, respectively, equal to 1, 10 and 1000 for the constant heat source. However, for the case 2, the maximum influence radial zone is 10 and it is happing at $t = 10$. This behavior has been also observed in the numerical model presented by Ghasemi-Fare and Basu (2013, 2016, 2018). Figs. 6(a) and 9(a) determine that soil temperature increments at both $z = 10$, and 15 are equal. The figures show soil temperature increases with depth and then close to the bottom of the heat source

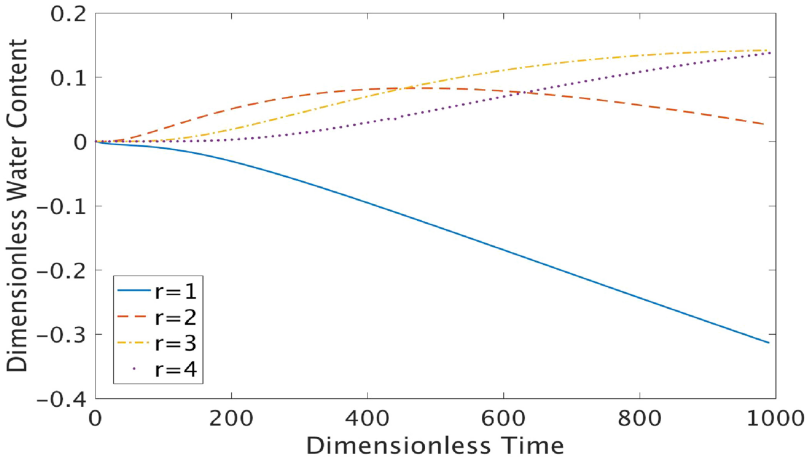

Fig. 10. Variation of water content with time at $z = 10$ and four different radiuses for case 1.

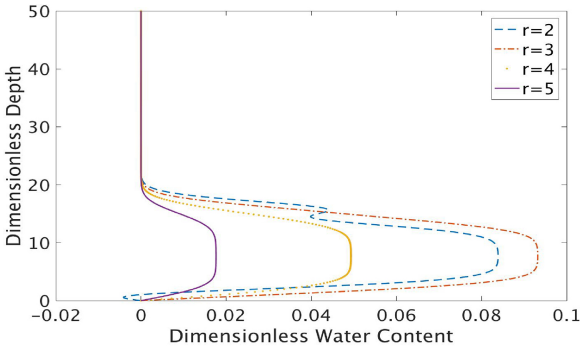

(a) At $t = 500$ and four different radiuses

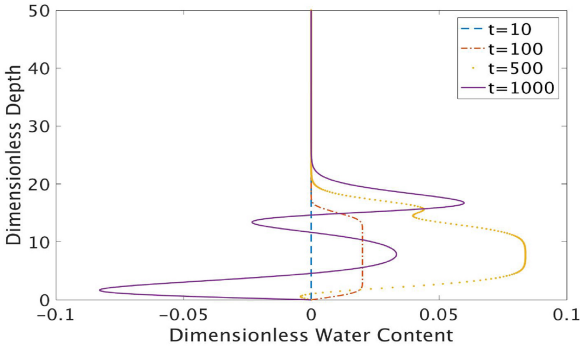

(b) At $r = 2$ and four different times

Fig. 11. Variation of water content with depth for case 1.

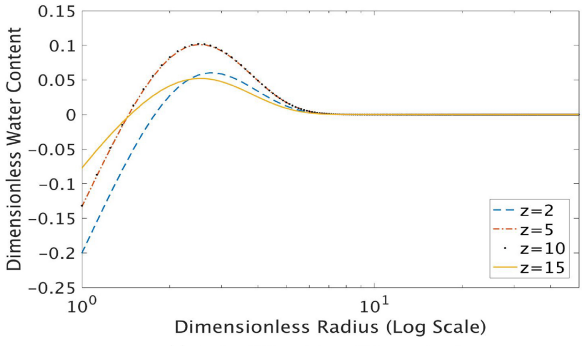

(a) At $t = 500$ and four different depths

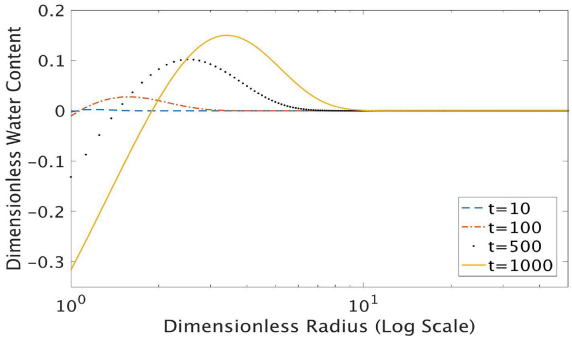

(b) At $z = 10$ and four different times

Fig. 12. Variation of water content with radius for case 1.

temperature starts to drop. Results confirm that the heat transfer in an unsaturated medium is mostly a radial phenomenon.

Fig. 7 illustrates the variation of temperature with time at five different locations for case 2. According to the figure, the temperature at each point gradually increases with time and reaches to the maximum value, and then it starts to decrease to get back to the initial condition. As it can be seen in the figure, zones closer to the heat source reach to the maximum value faster and there is a time lag for the farther zones. By comparing Figs. 4 and 7 it can be seen that temperature in case 1 increases from $t = 1$ to $t = 1000$, however, in case 2 maximum soil temperature at different locations occurred at different time steps. The delay in maximum soil temperature can be clearly seen in Fig. 7 where the maximum soil temperature for $r = 2$, and $r = 5$, respectively, occure at $t = 2$, and $t = 10$.

Figs. 10 and 13 present the variation of the water content with time at $z = 10$ for case 1, and case 2, respectively. As it can be seen in the figures, water content close to the heat source at $r = 1$ decreases with time; however, for $r = 2$, water content initially increases and then it starts to drop. This shows the moisture moves away from the heat source. According to the figures, for farther zones ($r = 4$) water content increases with time. This happens becasue, the water content is continuous in the domain, reduction in moisture content in the vicinity of the heat source increases its value in farther zones.

Figs. 11 and 14 indicate the variation of volumetric water content with depth for Case 1 and 2, respectively. Figs. 11(a) and 14(a) show the variation of the water content with depth at $t = 500$. The figures show moisture content is almost identical along the depth of the heat source at $t = 500$. It is interesting to note that water content is higher for $r = 3$ compare to $r = 2$ and 4, at $t = 500$. This shows the moisture flows away from the heat source and the maximum reaches to $r = 3$ at $t = 500$.

Figs. 11(b) and 14(b) present the changes in moisture content with depth at $r = 2$ for different time steps. The results show that the water

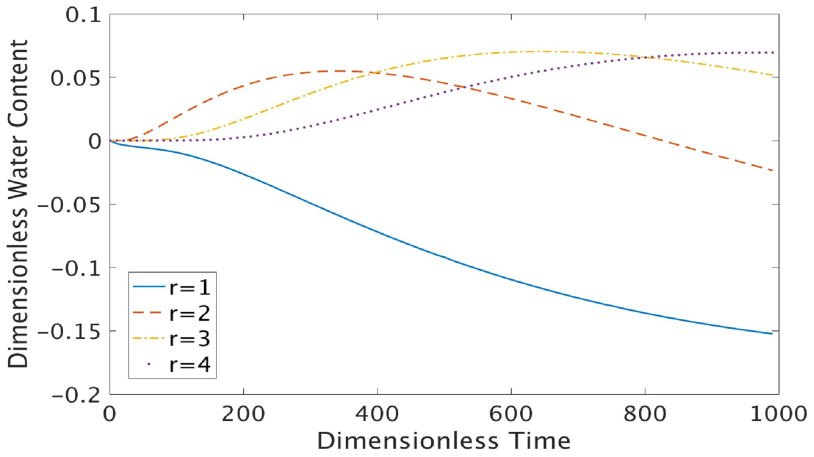

Fig. 13. Variation of water content with time at $z = 10$ and four different radiuses for case 2.

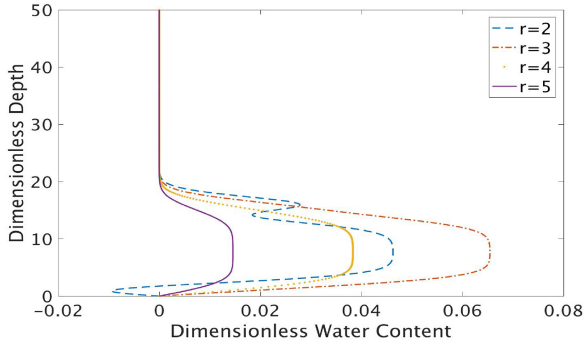

(a) At $t = 500$ and four different radiuses

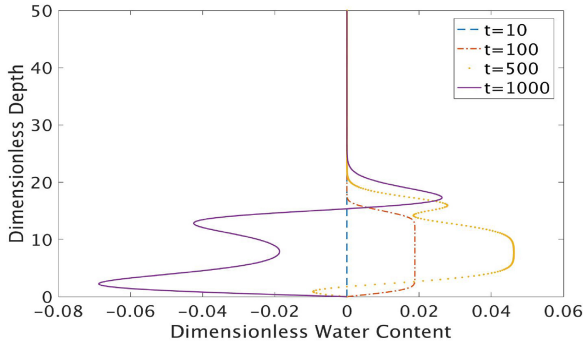

(b) At $r = 2$ and four different times

Fig. 14. Variation of water content with depth for case 2.

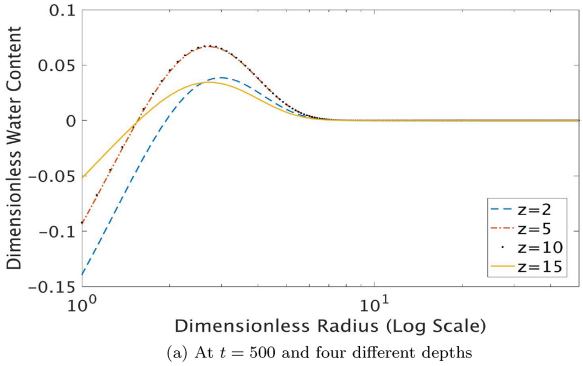

(a) At $t = 500$ and four different depths

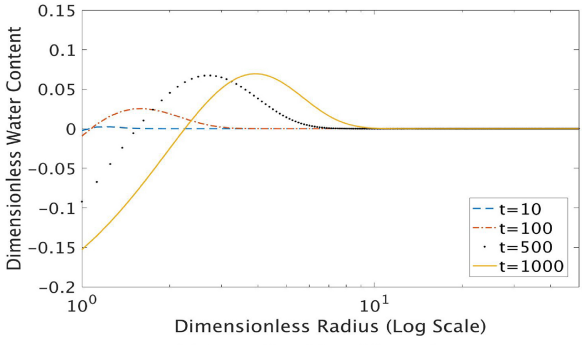

(b) At $z = 10$ and four different times

Fig. 15. Variation of water content with radius for case 2.

content is almost same as the initial condition at $t = 10$. This demonstrates that the moisture movement takes more time and it starts with some time lag after temperature changes in the soil media. According to the results presented in Figs. 11(b) and 14(b) moisture content varies differently in depth for longer time steps (e.g., $t = 1000$). The reductions in water content are different at $z = 2$, 5, and 13. This confirms the presence of the vortex flow in unsaturated medium and demonstrates that thermally induced moisture movement is not a radial phenomenon. The results presented here is compatible with the results from advanced numerical models (Ghasemi-Fare and Basu, 2018, 2017) while the closed form solution in this paper can be used easily with almost no computational cost. Note, this behavior has not been shown analytically in literature.

Figs. 12 and 15 present the water content variations with radius for case 1, and 2. Temperature increments close to the heat source results in moisture movement from zones close to the heat source to farther zones (from higher temperature to lower temperature). Figs. 12(a) and 15(a) clearly show water content is lower close to the heat source, and reaches to a maximum value farther from the heat source. However, there is always a zone far from the heat source in which the water content is constant. The figure shows the influence zone at $t = 500$ is $r = 6$ for all the depths. However, the influence zone depends on the time step and according to Figs. 12(b) and 15(b) the influence zone is expanding and reaches to $r = 10$ for the current study in which the

Table 4
Values of T and θ for different values of m, n, p and q.

T and θ	Values of m, n, p and q		
	1 to 20	1 to 100	1 to 200
T for $\nu = 0$	3.1522	1.5518	1.5520
T for $\nu = -0.5$	2.4507	1.2996	1.3018
θ for $\nu = 0$	0.1631	0.0829	0.0837
θ for $\nu = -0.5$	0.0798	0.0454	0.0461

temperature reaches to nearly a steady state condition at $t = 1000$. According to Figs. 12 and 15, as expected, the reduction in moisture content are higher for case 1. The reason is temperature increments are higher surrounding the constant heat source. We should also note that the raise in water content for farther zones are also higher in case 1 compare to case 2. This can be expected because as mentioned earlier, the water content is continuous in the domain and higher reduction close to the heat source results in higher water content in farther zones. The closed form solution in this study can be used to predict both temperature and water content in the porous media surrounding any heat sources such as geothermal piles. The equations and the provided solution will be a good source for the validation of numerical models.

7. Potential error sources

As mentioned, the employed methods in this research are exact. Therefore, Eqs. (33) and (49) are exact closed form solutions of Eqs. (9) and (11), respectively. But there might be a truncation error due to cutting the parameters of m, n, p and q. According to the solutions, this four parameters changes from 1 to infinity. However, in this study, changes from 1 to 100 were considered. For different values of above mentioned parameters, Table 4 indicates the values of temperature and volumetric water content at $z = 10$, $r = 2$, and $t = 1$ and 500 respectively.

As can be seen, considering mentioned parameters from 1 to a value greater than 100 have negligible effects on the results.

8. Conclusion

Analyzing the hydrothermal behavior of porous media and modeling both heat and water flow is a complex problem. Such problems are usually solved using numerical methods. However, easy to use equations considering some simplifying assumptions are powerful tools to do the preliminary study and design the complex problems. Besides, numerical models have high computational cost. The analytical solutions can be also used to validate numerical models. In this paper, a convenient analytical solution is developed to study the heat and water flow surrounding an energy pile in an unsaturated soil. The heat source is used to represent the energy pile. The Green's function method is employed to analytically predict the soil hydrothermal behavior. The fundamental proposed solution can be employed to study the effects of soil hydrothermal parameters on temperature and volumetric water content profiles in unsaturated soil media. It was observed that at a certain time, the water content reduces for the zones close to the energy pile while it increases for farther zones (e.g., $r = 3$ and $r = 4$). It was also observed that the maximum changes in water content happen at the same depth which shows the maximum temperature interments. It is interesting to note that the water content in soil media shows a dynamic response for longer time steps. The results confirm the presence of a vortex which makes different volumetric moisture content along the depth at $t = 1000$. The results showed the influence zone in which temperature increases during the thermal loading are, respectively, $r = 30$, and $r = 10$ for the constant heat source, and a heat source which attenuates with time. While the influence zone in which the moisture content changes is independent of the heat source type and is equal to $r = 10$. However the magnitude of volumetric moisture content reductions and increments, are greater in case 1 in which temperature gradient is higher.

Acknowledgements

The Second author would like to gratefully acknowledge the financial support by the National Science Foundation under the Grant No. CMMI-1804822.

References

Ã-zisik, M.N., Özışık, M.N., 1993. Heat Conduction. John Wiley & Sons.
Baggio, P., Bonacina, C., Schrefler, B., 1997. Some considerations on modeling heat and mass transfer in porous media. Transp. Porous Media 28 (3), 233–251. https://doi.org/10.1023/A:100652572.
Beier, R.A., Smith, M.D., Spitler, J.D., 2011. Reference data sets for vertical borehole ground heat exchanger models and thermal response test analysis. Geothermics 40 (1), 79–85.
Chen, G., Ledesma, A., 2007. Coupled solution of heat and moisture flow in unsaturated clay barriers in a repository geometry. Int. J. Numer. Anal. Methods Geomech. 31 (8), 1045–1065. https://doi.org/10.1002/nag.565.
De Vries, D., 1958. Simultaneous transfer of heat and moisture in porous media, Eos. Trans. Am. Geophys. Union 39 (5), 909–916. https://doi.org/10.1029/TR039i005p00909.
Eskilson, P., Claesson, J., 1988. Simulation model for thermally interacting heat extraction boreholes. Numer. Heat Transf. 13 (2), 149–165. https://doi.org/10.1080/10407788808913609.
Ghasemi-Fare, O., Basu, P., 2013. An Annular Cylinder Source Model for Heat Transfer Through Energy Piles, TRB 92nd Annual Meeting.
Gao, Y., Fan, R., Li, H., Liu, R., Lin, X., Guo, H., Gao, Y., 2016. Thermal performance improvement of a horizontal ground-coupled heat exchanger by rainwater harvest. Energy Build. 110, 302–313. https://doi.org/10.1016/j.enbuild.2015.10.030.
Gatmiri, B., Delage, P., 1997. A formulation of fully coupled thermal-hydraulic-mechanical behaviour of saturated porous media-numerical approach. Int. J. Numer. Anal. Methods Geomech. 21 (3), 199–225. https://doi.org/10.1002/(SICI)1096-9853(199703)21:3<199::AID-NAG865>3.0.CO;2-M.
Gatmiri, B., Jabbari, E., 2005a. Time-domain green's functions for unsaturated soils. Part I: Two-dimensional solution. Int. J. Solids Struct. 42 (23), 5971–5990. https://doi.org/10.1016/j.ijsolstr.2005.03.039.
Gatmiri, B., Jabbari, E., 2005b. Time-domain green's functions for unsaturated soils. Part II: Three-dimensional solution. Int. J. Solids Struct. 42 (23), 5991–6002. https://doi.org/10.1016/j.ijsolstr.2005.03.040.
Gawin, D., Schrefler, B.A., Galindo, M., 1996. Thermo-hydro-mechanical analysis of partially saturated porous materials. Eng. Comput. 13 (7), 113–143. https://doi.org/10.1108/02644409610151584.
Ghasemi-Fare, O., Basu, P., 2013. A practical heat transfer model for geothermal piles. Energy Build. 66, 470–479. https://doi.org/10.1016/j.enbuild.2013.07.048.
Ghasemi-Fare, O., Basu, P., 2016. Predictive assessment of heat exchange performance of geothermal piles. Renew. Energy 86, 1178–1196. https://doi.org/10.1016/j.renene.2015.08.078.
Ghasemi-Fare, O., Basu, P., 2017. Role of thermally-induced buoyant flow in altering energy harvesting using geothermal piles. Geotech. Front. 113–123.
Ghasemi-Fare, O., Basu, P., 2018. Influences of ground saturation and thermal boundary condition on energy harvesting using geothermal piles. Energy Build. 165, 340–351. https://doi.org/10.1016/j.enbuild.2018.01.030.
Hartley, J., Black, W., 1981. Transient simultaneous heat and mass transfer in moist, unsaturated soils. J. Heat Transf. 103 (2), 376–382. https://doi.org/10.1115/1.3244469.
Jeffrey, A., 2001. Advanced Engineering Mathematics. Elsevier.
Khalili, N., Loret, B., 2001. An elasto-plastic model for non-isothermal analysis of flow and deformation in unsaturated porous media: formulation. Int. J. Solids Struct. 38 (46–47), 8305–8330. https://doi.org/10.1016/S0020-7683(01)00081-6.
Lamarche, L., Beauchamp, B., 2007. New solutions for the short-time analysis of geothermal vertical boreholes. Int. J. Heat Mass Transf. 50 (7–8), 1408–1419. https://doi.org/10.1016/j.ijheatmasstransfer.2006.09.007.
Lamarche, L., 2011. Analytical g-function for inclined boreholes in ground-source heat pump systems. Geothermics 40 (4), 241–249. https://doi.org/10.1016/j.geothermics.2011.07.006.
Li, X., Zhao, J., Zhou, Q., 2005. Inner heat source model with heat and moisture transfer in soil around the underground heat exchanger. Appl. Therm. Eng. 25 (10), 1565–1577. https://doi.org/10.1016/j.applthermaleng.2004.10.002.
Maghoul, P., Gatmiri, B., Duhamel, D., 2009. 3d transient fundamental solution of multiphase porous media under heating. In: 4th Biot Conference on Poromechanics. New York, USA, 8–10 June. pp. 911–916.
Man, Y., Yang, H., Diao, N., Liu, J., Fang, Z., 2010. A new model and analytical solutions for borehole and pile ground heat exchangers. Int. J. Heat Mass Transf. 53 (13–14), 2593–2601. https://doi.org/10.1016/j.ijheatmasstransfer.2010.03.001.
Olivella, S., Gens, A., 2000. Vapour transport in low permeability unsaturated soils with capillary effects. Transp. Porous Media 40 (2), 219–241.
Pan, E., 1999. Green's functions in layered poroelastic half-spaces. Int. J. Numer. Anal. Methods Geomech. 23 (13), 1631–1653. https://doi.org/10.1002/(SICI)1096-9853(199911)23:13<1631::AID-NAG60>3.0.CO;2-Q.
Philip, J., De Vries, D., 1957. Moisture movement in porous materials under temperature gradients, Eos. Trans. Am. Geophys. Union 38 (2), 222–232. https://doi.org/10.1029/TR038i002p00222.
Rockhold, M.L., Simmons, C.S., Fayer, M.J., 1997. An analytical solution technique for one-dimensional, steady vertical water flow in layered soils. Water Resour. Res. 33 (4), 897–902. https://doi.org/10.1029/96WR03746.
Selvadurai, A., 2007. The analytical method in geomechanics. Appl. Mech. Rev. 60 (3), 87–106. https://doi.org/10.1115/1.2730845.
Shao, M., Horton, R., Jaynes, D., 1998. Analytical solution for one-dimensional heat conduction-convection equation. Soil Sci. Soc. Am. J. 62 (1), 123–128. https://doi.org/10.2136/sssaj1998.03615995006200010016x.
Spitler, J.D., Javed, S., Ramstad, R.K., 2016. Natural convection in groundwater-filled

boreholes used as ground heat exchangers. Appl. Energy 164, 352–365. https://doi.org/10.1016/j.apenergy.2015.11.041.

Taguchi, I., Kurashige, M., 2002. Fundamental solutions for a fluid-saturated, transversely isotropic, poroelastic solid. Int. J. Numer. Anal. Methods Geomech. 26 (3), 299–321. https://doi.org/10.1002/nag.202.

Taylor, S.A., Cary, J.W., 1964. Linear equations for the simultaneous flow of matter and energy in a continuous soil system 1. Soil Sci. Soc. Am. J. 28 (2), 167–172. https://doi.org/10.2136/sssaj1964.03615995002800020013x.

Thomas, H., 1985. Modelling two-dimensional heat and moisture transfer in unsaturated soils, including gravity effects. Int. J. Numer. Anal. Methods Geomech. 9 (6), 573–588. https://doi.org/10.1002/nag.1610090606.

Wu, W., Li, X., Charlier, R., Collin, F., 2004. A thermo-hydro-mechanical constitutive model and its numerical modelling for unsaturated soils. Comput. Geotech. 31 (2), 155–167. https://doi.org/10.1016/j.compgeo.2004.02.004.

Zeng, H., Diao, N., Fang, Z., 2002. A finite line-source model for boreholes in geothermal heat exchangers. Heat Transf.-Asian Res. 31 (7), 558–567. https://doi.org/10.1002/htj.10057.

Zeng, H., Diao, N., Fang, Z., 2003. Heat transfer analysis of boreholes in vertical ground heat exchangers. Int. J. Heat Mass Transf. 46 (23), 4467–4481. https://doi.org/10.1016/S0017-9310(03)00270-9.